

From WMAP to PLANCK: Exact reconstruction of 4- and 5-dimensional inflationary potential from high precision CMB measurements

L.A. Popa¹, N. Mandolesi², A. Caramete¹, C. Burigana²

¹ *Institutul de Științe Spațiale București-Măgurele, Ro-077125 România*

² *INAF/IASF, Istituto di Astrofisica Spaziale e Fisica Cosmica Bologna, I-40129, Italia*

lpopa@venus.nipne.ro

ABSTRACT

We make a more general determination of the inflationary observables in the standard 4-D and 5-D single-field inflationary scenarios, by the exact reconstruction of the dynamics of the inflation potential during the observable inflation with minimal number of assumptions: the computation does not assume the slow-roll approximation and is valid in all regimes if the field is monotonically rolling down its potential.

We address higher-order effects in the standard and braneworld single-field inflation scenarios by fitting the Hubble expansion rate and subsequently the inflationary potential directly to WMAP5+SN+BAO and Planck-like simulated datasets.

Making use of the *Hamilton-Jacobi* formalism developed for the 5-D single-field inflation model, we compute the scale dependence of the amplitudes of the scalar and tensor perturbations by integrating the exact mode equation. The solutions in 4-D and 5-D inflation scenarios differ through the dynamics of the background scalar field and the number of e -folds assumed to be compatible with the observational window of inflation.

We analyze the implications of the theoretical uncertainty in the determination of the reheating temperature after inflation on the observable predictions of inflation and evaluate its impact on the degeneracy of the standard inflation consistency relation.

We find that the detection of tensor perturbations and the theoretical uncertainties in the inflationary observable represent a significant challenge for the future PLANCK CMB measurements: distinguishing between the observational signatures of the standard and braneworld single-field inflation scenarios.

This work have been done in the frame of PLANCK Core Team activities.

Subject headings: cosmology: cosmic microwave background, cosmological parameters, early universe, observations

1. Introduction

The primary goal of particle cosmology is to obtain a concordant description of the origin and early evolution of the Universe, consistent with both unified field theory and astrophysical and cosmological measurements.

Inflation is the most simple and robust theory able to explain the astrophysical and cosmological observations, providing at the same time self-consistent primordial initial conditions (Starobinsky 1979; Guth 1981; Sato 1981; Albrecht & Steinhardt 1982; Linde 1983 ; Linde 1983) and the mechanisms for quantum generation of the scalar and tensor perturbations (Mukhanov & Chibisov 1981; Hawking 1982; Starobinsky 1982; Guth & Pi 1982; Bardeen et al. 1983; Abbott & Wise 1984).

In the simplest class of inflationary models, inflation is driven by a single scalar field ϕ (inflaton) with some potential $V(\phi)$, minimally coupled to Einstein gravity. The perturbations are predicted to be adiabatic, nearly scale-invariant and Gaussian distributed, resulting in an effectively flat Universe. At the leading-order in slow-roll approximation (Steinhardt & Turner 1984; Salopek & Bond 1990; Liddle et al. 1994) the amplitudes of scalar and tensor perturbations on a specified comoving wavenumber k , are related through the consistency equation:

$$\frac{A_T^2}{A_S^2} = -\frac{n_T}{2}, \quad (1)$$

where: $A_S^2 \propto k^{n_S-1}$ and $A_T^2 \propto k^{n_T}$ are the amplitudes of scalar and tensor perturbations respectively and n_S and n_T are their tilts. The consistency equation may be regarded as an independent test of single-field inflationary models as it does not depend on the specific functional form of the inflation potential.

Recent WMAP 5-year CMB measurements, alone (Dunkley et al. 2009) or complemented with other cosmological datasets (Komatsu et al. 2009), support the standard inflationary predictions of a nearly flat Universe with adiabatic initial density perturbations.

In particular, the detected anti-correlations between temperature and E-mode polarization anisotropy on degree scales (Nolta et al. 2009) provide strong evidence for correlation on length scales beyond the Hubble radius.

Despite the successes of inflationary cosmology, recent proposals in theoretical physics motivated by the developments in superstring and M-theory (Horava & Witten 1996), suggest that our four-dimensional Universe could lie on a brane embedded in higher-dimensional

space-time (see e.g. Rubakov 2001, Maartens 2004 and references therein).

In particular, in the type II Randall-Sundrum model (RSII) (Randall & Sundrum 1999a; Randall & Sundrum 1999b) our four-dimensional (4-D) Universe is a brane with positive tension λ embed in a five-dimensional (5-D) anti-de Sitter space-time (AdS_5). At sufficiently low energies ($\rho \ll \lambda$) the standard cosmic behavior is recovered and the primordial nucleosynthesis constraint is satisfied, provided that $\lambda \geq (1 \text{ MeV})^4$.

The simplest way to realize inflation in RSII model is to have a single scalar field confined to the brane and only gravity in the bulk (Maartens et al. 2000). In this case the Friedmann equation is modified so that Hubble parameter $H \propto \rho$ rather than $H \propto \rho^{1/2}$ as in 4-D case, leading to significant modifications of the amplitudes and scale dependencies of scalar and tensor perturbations (Binetruy et al. 2000).

The observational constraints on inflationary parameters in 5-D scenario, made in general by using the slow-roll (SR) approximation in the high energy regime ($\rho \gg \lambda$), show that to the leading order in SR the consistency equation has precisely the same form as in the standard 4-D scenario, the relationship between inflationary observables being independent on the brane tension (Tsujiikawa & Liddle 2004; Seery & Taylor 2005).

The degeneracy of consistency equation was associated with the fact that 5-D inflationary observables smoothly approach their 4-D counterparts as the brane decouples from the bulk approaching the low energy regime ($\rho \ll \lambda$). The main assumption made by these works is that the back-reaction due to metric perturbation in the bulk can be neglected. This assumption is valid to the leading-order in slow-roll approximation, as the coupling between inflation fluctuations and metric perturbation vanishes.

Recently it was shown (Koyama et al. 2004; Koyama et al. 2005a; Koyama et al. 2005b) that the sub-horizon inflation fluctuations on the brane excite an infinite ladder of Kaluza-Klein modes of the bulk metric perturbations to second-order in slow-roll parameters. If the back-reaction is taken into account, the amplitude of the scalar perturbations receives second-order slow-roll corrections in addition to Stewart-Lyth corrections (Stewart & Lyth 1993), of the same order of magnitude (Koyama et al. 2008). The degeneracy of consistency equations does not hold when the second-order corrections in SR expansion for perturbations are included (Calcagni 2003; Calcagni 2004; Ramirez & Liddle 2004; Seery & Taylor 2005).

One of the most anticipated results of forthcoming high precision CMB experiments is probing the physics of inflation and in particular the reconstruction of the inflation potential. In order to have a robust interpretation of upcoming observations it is imperative to understand how the reconstruction process may be affected by the degeneracy of the inflationary observables. In this paper we aim to make a more general determination of the inflationary observables in 4-D and 5-D inflationary scenarios, by exact reconstruction of the dynamics of the inflation potential during the observable inflation with minimal number of assumptions

(Lesgourgues et al. 2008; Hamann et al. 2008).

Taking the advantage of the formalism developed for the standard single-field inflation (Peiris et al. 2003; Peiris & Easther 2006a; Peiris & Easther 2006b; Martin & Ringeval 2006; Lesgourgues et al. 2008; Alabidi & Lidsey 2008), we carry out similar calculations for 5-D inflation models by fitting the Hubble function, $H(\phi)$, and subsequently the inflationary potential, $V(\phi)$, directly to WMAP 5-year data (Dunkley et al. 2009; Komatsu et al. 2009) complemented with geometric probes from the Type Ia supernovae (SN) distance-redshift relation and the baryon acoustic oscillations (BAO) measurements and Planck-like CMB anisotropy simulated data.

Our specific goal is to address higher-order effects in the standard and braneworld single-field inflation models and to analyze the sensitivity of the present and future CMB temperature and polarization measurements to discriminate between them.

The paper is organized as follows. In Section 2 we review the Hamilton-Jacobi formalisms for 4-D and 5-D single-field inflation models. In Section 3 we compute the scalar and tensor perturbation spectra for standard and braneworld single-field inflation models by using the exact mode equation. In Section 4 we present the implementation of the Markov Chain Monte-Carlo methodology and describe the datasets involved in our analysis. Section 5 is dedicated to the analysis and the interpretation of our results: we present the derived bounds on the inflationary parameters, Hubble Slow-Roll parameters and the magnitude, slope and curvature of the inflationary potentials obtained from the fits of 4-D and 5-D single-field inflation models to our datasets and analyze the possibility to disentangle between standard and braneworld scenarios by using the future PLANCK high precision CMB measurements. In Section 6 we draw our conclusions.

Throughout the paper m_4 and m_5 denote the corresponding 4-D and 5-D Planck mass scales and we have set $Gm_4^2 = \hbar = c = 1$. Also, we denote by dot the derivative with respect to the time and by prime the derivative with respect to the scalar field.

2. The four- and five-dimensional Hamilton-Jacobi formalism

2.1. The 4-D single-field inflation case

The Hubble Slow-Roll (HSR) formalism for the standard single-field inflation was set down in detail by Liddle, Parsons & Barrow (1994).

The Friedmann equation in zero-curvature Universe is given by:

$$H_{4D}^2 = \frac{8\pi}{3m_4^2}\rho, \quad (2)$$

where: $H \equiv \dot{a}/a$ is the Hubble parameter, a is the cosmological scale factor, $\rho = V + \dot{\phi}^2/2$ is the total energy density, where $V(\phi)$ and $\dot{\phi}^2/2$ are the potential and kinetic energy density terms respectively. Since the dark energy contribution is strongly suppressed by the exponential expansion during inflation (Maartens et al. 2000; Langlois et al. 2001), we set to zero the dark energy term in the above equation.

The equation of motion for the scalar field is given by:

$$\ddot{\phi} + 3H\dot{\phi} = -V'. \quad (3)$$

Eqs. (2) and (3) can be written in the *Hamilton-Jacobi* form, allowing to consider inflation in terms of $H(\phi)$ rather than $V(\phi)$ (Liddle et al. 1994; Kinney 2002; Easter & Kinney 2003; Peiris et al. 2003; Kinney et al. 2004):

$$H'(\phi)a'(\phi) = -\frac{4\pi}{m_4^2}H(\phi)a(\phi), \quad (4)$$

$$\dot{\phi} = -\frac{m_4^2}{4\pi}H'(\phi), \quad (5)$$

$$[H'(\phi)]^2 - \frac{12\pi}{m_4^2}H^2(\phi) = -\frac{32\pi^2}{m_4^4}V(\phi). \quad (6)$$

For any value of $H(\phi)$ Eq. (6) can be used to find $V(\phi)$ while Eqs. (4) and (5) allow to convert ϕ -dependence into time-dependence.

In the standard 4-D inflation the first three HSR parameters are given (Liddle et al. 1994):

$$\epsilon_H = \frac{m_4^2}{4\pi} \frac{H'^2(\phi)}{H^2(\phi)}, \quad (7)$$

$$\eta_H(\phi) = \frac{m_4^2}{4\pi} \frac{H''(\phi)}{H(\phi)}, \quad (8)$$

$$\zeta_H^2(\phi) = \frac{m_4^4}{16\pi^2} \frac{H'(\phi)H'''(\phi)}{H(\phi)}. \quad (9)$$

The dependence of $V(\phi)$ on $H(\phi)$ can be obtain by substituting ϵ_H into Eq. (6) leading to:

$$\frac{8\pi}{3m_4^2}V(\phi) = H^2(\phi) \left[1 - \frac{1}{3}\epsilon_H(\phi) \right]. \quad (10)$$

The HSR formalism ensures that the condition for inflation to occur is precisely $\epsilon_H < 1$ and inflation ends exactly when $\epsilon_H = 1$.

2.2. The 5-D single-field inflation case

In the 5-D inflation case the Eq.(2) receives an additional term quadratic in energy density:

$$H_{5D}^2 = \frac{8\pi}{3m_4^2} \rho \left(1 + \frac{\rho}{2\lambda} \right), \quad (11)$$

where: $\rho = V + \dot{\phi}^2/2$ is the total energy density and λ is the brane tension. The scalar field ϕ is assumed to obey the same equation of motion as in 4-D standard inflation as given by Eq.(3). In the low-energy regime ($\rho \ll \lambda$) the quadratic term in Eq.(11) can be neglected and one recover the behavior of the 4-D standard cosmology. In high-energy regime ($\rho \gg \lambda$) the deviation from the standard expansion changes the amplitudes and scale-dependence of cosmological perturbations.

Hereafter we will make use of the approach developed by Hawkins and Lidsey who derived a general formalism for 5-D inflation case valid in all regimes, having many of the properties of the *Hamilton-Jacobi* formalism in 4-D standard inflation (Hawkins & Lidsey 2001; Hawkins & Lidsey 2003). They defined a quantity $y(\phi)$ with the same role as $H(\phi)$ in the case of 4-D standard inflation:

$$y^2(\phi) = \frac{\rho/2\lambda}{1 + \rho/2\lambda}, \quad (12)$$

with the inverse relation given by:

$$\rho = \frac{2\lambda y^2(\phi)}{1 - y^2(\phi)}. \quad (13)$$

In terms of $y(\phi)$ the Friedmann equation (11) reads as:

$$H_{5D}^2(y) = \frac{16\pi\lambda}{3m_4^2} \frac{y^2(\phi)}{(1 - y^2(\phi))^2}, \quad (14)$$

where the restriction $y^2 < 1$ is imposed, implying that $y(\phi)$ is proportional to $H(\phi)$ in the low-energy limit, $y \rightarrow 0$ ($\rho/\lambda \rightarrow 0$).

The Hamilton-Jacobi equations, analogues to Eqs. (4) - (6) for 4-D standard inflation are given by (Hawkins & Lidsey 2003; Ramirez & Liddle 2004):

$$y'(\phi)a'(\phi) = -\frac{4\pi}{m_4^2} y(\phi)a(\phi), \quad (15)$$

$$\dot{\phi} = -\left(\frac{\lambda m_4^2}{3\pi}\right)^{1/2} \frac{y'}{1 - y^2}, \quad (16)$$

$$H'(\phi) = -\frac{4\pi}{m_4^2} \frac{(1 + y^2)}{(1 - y^2)} \dot{\phi}, \quad (17)$$

and the dependence of $V(\phi)$ on $y(\phi)$ can be obtained by combining Eqs.(16) and (17) leading to:

$$V(\phi) = \frac{2\lambda y^2}{1-y^2} - \frac{\lambda m_4^2}{6\pi} \left(\frac{y'}{1-y^2} \right). \quad (18)$$

The first three HSR parameters in terms of $y(\phi)$ reads as (Ramirez & Liddle 2004):

$$\epsilon_H = \left(\frac{\lambda m_4^2}{3\pi} \right)^{1/2} \frac{y}{(1+y^2)} \frac{H'^2}{H^3}, \quad (19)$$

$$\eta_H = \left(\frac{\lambda m_4^2}{3\pi} \right)^{1/2} \left[\frac{y}{(1+y^2)} \frac{H''}{H^2} - \frac{4y^3}{(1+y^2)^3} \frac{H'^2}{H^3} \right], \quad (20)$$

$$\xi_H^2 = \frac{\ddot{\phi}}{H^2 \dot{\phi}} - \eta_H^2. \quad (21)$$

The above definitions of HSR parameters are valid in all regimes, generalizing the previous ones, preserving at the same time many of the inflation key properties: they are obtained by demanding the condition for inflation to occur precisely for $\epsilon_H < 1$ and to end exactly when $\epsilon_H = 1$. Also, they are preserving the lowest-order slow-roll definitions of the scalar spectral index, $n_S = 1 - 4\epsilon_H + 2\eta_H$, and of its running, $dn_S/d\ln k = 5\epsilon_H\eta_H - 4\epsilon_H^2 - 2\xi_H^2$.

3. The four- and five-dimensional exact mode equation

The scale dependence of the amplitudes of the scalar (S) and tensor (T) perturbations can be exactly obtained by integrating the mode equation (Mukhanov 1985; Mukhanov 1989):

$$u_k'' + \left(k^2 - \frac{z_{S,T}''}{z_{S,T}} \right) u_k = 0, \quad (22)$$

where primes denote the second derivatives with respect to the conformal time.

The numerical evaluation of the spectra involves solving Eq.(22) for each value of the wavenumber k , the evolution of $|u_k|/z_{S,T}$ to a constant value defining the observable power spectra $\mathcal{P}_{S,T}$. The solutions differ through the evolution of the background scalar field and the prior on the number of e -folds assumed to be compatible with the observational window of inflation.

3.1. The 4-D single-field inflation case

We compute the amplitudes of scalar and tensor perturbations by using the standard inflation numerical module from Lesgourgues et al. (2008). For each wavenumber k in a given

range the code integrates Eq.(22) in an observational inflationary window corresponding to a number of ΔN e -folds, imposing that k grows monotonically to the wavenumber k_* that leaves the Hubble radius when $\phi = \phi_*$, eliminating at the same time the models violating the condition for inflation ($\epsilon_H < 1$).

For the purpose of present analysis we reconstruct the Hubble expansion rate $H(\phi - \phi_*)$ from the data by using the Taylor expansion up to the cubic term:

$$H(\phi - \phi_*) = H_* + H'_*(\phi - \phi_*) + \frac{1}{2}H''_*(\phi - \phi_*)^2 + \frac{1}{6}H'''_*(\phi - \phi_*)^3, \quad (23)$$

equivalent to keeping the first three HSR parameters. We consider wavenumbers in the range $[5 \times 10^{-6} - 5] \text{ Mpc}^{-1}$ needed to numerically derive the CMB angular power spectra and the Hubble crossing scale $k_* = 0.01 \text{ Mpc}^{-1}$.

The analysis however depends on the prior on the interval over which the dynamics of the background field is tracked. Actually, the standard inflation numerical module integrates Eq.(22) from the time at which $k/aH = 50$ until $d \ln \mathcal{P}_{S,T}/d \ln a < 3 \times 10^{-3}$. This choice ensures that inflation started enough time before the observational range and ends ($\epsilon_H = 1$) enough time after the smallest observable scale leaves the Hubble horizon scale $k_* = 0.01 \text{ Mpc}^{-1}$, leading at the same time to an accuracy of $\sim 0.1\%$ in final power spectra amplitudes, that is smaller than the expected sensitivity of CMB data (Hamann et al. 2008). For these reasons we choose to keep this time integration window for our computation.

The power spectra of scalar and tensor perturbations are obtained as (Stewart & Lyth 1993; Copeland et al. 1994):

$$\mathcal{P}_S(k) = \frac{k^3}{2\pi^2} \left(\frac{H}{\dot{\phi}} \right)^2 \frac{|u_k|^2}{a^2}, \quad \mathcal{P}_T(k) = \frac{16k^3}{\pi m_4^2} \frac{|u_k|^2}{a^2}, \quad (24)$$

where $z_S = a\dot{\phi}/H$ for scalars, $z_T = a$ for tensors and the temporal evolution of the scalar field is given by Eq.(5).

3.2. The 5-D single-field inflation case

There is supporting evidence for the use of the exact mode Eq.(22) in braneworld context, because its derivation does not involve the Friedmann equation (Liddle & Lyth 2000). We modify the standard inflation module from Lesgourgues et al. (2008) to compute the power spectra of scalar and tensor perturbations for the single-field braneworld inflation.

As in the case of 4-D standard inflation, the Hubble expansion rate $H(\phi - \phi_*)$ is obtained from the data by the Taylor expansion up to the cubic term the neighborhood of the pivot scale $k_*=0.01 \text{ Mpc}^{-1}$.

For each wavenumbers k in the range $[5 \times 10^{-6} - 5]$ Mpc^{-1} we integrate Eq.(22) keeping the same time integration window as in the 4-D inflation case. In this way, the identical scales (wavenumbers) encompass the same number of e -folds at Hubble radius crossing k_* in both 4-D and 5-D inflationary scenarios ensuring the same accuracy in the reconstruction of the inflationary potential (Kinney 2002). As in the 4-D case we impose the condition that each mode k grows monotonically to the wavenumber k_* and we eliminate those models violating the condition for inflation ($\epsilon_H < 1$).

Taking $z_S = aH/\dot{\phi}$ for scalars, $z_T = a$ for tensors and the evolution of the scalar field given by Eq.(16), the power spectra of scalar and tensor perturbations are then obtained as (Ramirez & Liddle 2004; Koyama et al. 2008):

$$\mathcal{P}_S(k) = \frac{k^3}{25\pi^2} \left(\frac{H}{\dot{\phi}}\right)^2 \frac{|u_k|^2}{a^2} [1 + \mathcal{K}(\beta^2)], \quad \mathcal{P}_T(k) = \frac{16k^3}{\pi m_4^2} \frac{|u_k|^2}{a^2}. \quad (25)$$

The correction $\mathcal{K}(\beta^2)$ to $\mathcal{P}_S(k)$ is solely due to the coupling between the inflation field and the bulk metric perturbations (Koyama et al. 2005a; Koyama et al. 2005b; Koyama et al. 2008). For each wavenumber k we obtained $\mathcal{K}(\beta^2)$ by numerical computation (Koyama et al. 2008), taking β^2 given by (Koyama et al. 2008):

$$\beta^2 = \frac{1}{3}\epsilon_H \left[1 + \left(\frac{\mu}{H}\right)^2\right]^{-1/2}. \quad (26)$$

One should note that, although the power spectra of the tensor perturbations in 4-D and 5-D inflation have the same form, they differ through their dependencies on the cosmological scale factor $a(\phi)$ and on the conformal time: $\eta(a) = \int da/a^2 H$.

Defining the amplitudes of scalar and tensor power spectra as (Copeland et al. 1994)¹: $A_S(k) = 2\mathcal{P}_S^{1/2}(k)/5$ and $A_T(k) = \mathcal{P}_T^{1/2}(k)/10$, the scalar and tensor spectral indexes $n_{S,T}$ and the running of scalar tilt α_S at the Hubble radius crossing $k = aH$ are defined as usual by:

$$n_S - 1 \equiv \left. \frac{d \ln A_S^2}{d \ln k} \right|_{k=aH} \quad n_T \equiv \left. \frac{d \ln A_T^2}{d \ln k} \right|_{k=aH} \quad \alpha_S \equiv \left. \frac{d n_S}{d \ln k} \right|_{k=aH}. \quad (27)$$

4. The Markov Chain Monte Carlo methodology

We use the Markov Chain Monte Carlo (MCMC) technique to reconstruct the inflationary potential and to derive constraints on the inflationary observables in the 4-D inflation

¹The normalization of $\mathcal{P}_S(k)$ ensures that A_S coincides precisely with the density contrast δ_H at Hubble radius crossing as defined by Liddle and Lyth (Liddle & Lyth 2000). The normalization of $\mathcal{P}_T(k)$ is then chosen so that $\epsilon_H = A_T^2/A_S^2$.

and 5-D single-field inflation models by using the WMAP 5-year data (Dunkley et al. 2009; Komatsu et al. 2009) complemented with geometric probes from the Type Ia supernovae (SN) distance-redshift relation and the baryon acoustic oscillations (BAO).

The SN distance-redshift relation has been studied in detail in the recent unified analysis of the published heterogeneous SN data sets - the Union Compilation08 (Kowalski et al. 2008). The BAO in the distribution of galaxies are extracted from the Sloan Digital Sky Surveys (SDSS) and Two Degree Field Galaxy Redshift Survey (2DFGRS) (Percival et al. 2007). The CMB, SN and BAO data (WMAP5+SN+BAO) are combined by multiplying the likelihoods. We decided to use these measurements especially because we are testing models deviating from the standard Friedmann expansion. These datasets properly enables us to account for any shift of the CMB angular diameter distance and of the expansion rate of the Universe.

For the forecast from PLANCK-like simulated data we use the CMB temperature (T) and polarization (P) power spectra of our fiducial cosmological model and the expected experimental characteristics of the PLANCK frequency channels given in Table 1 (Mandolesi et al. 2009; PLANCK Consortia 2005). For each frequency channel we consider an homogeneous detector noise with the power spectrum given by (Perotto et al. 2006; Popa & Vasile 2007):

$$N_{l,\nu}^c = (\theta_b \Delta_a)^2 \exp^{l(l+1)\theta_b^2/8 \ln 2} \quad c \in (T, P), \quad (28)$$

where ν is the frequency of the channel, θ_b is the FWHM of the beam and Δ_c are the corresponding sensitivities per pixel. The global noise of the experiment is obtained as:

$$N_l^c = \left[\sum_{\nu} (N_{l,\nu}^c)^{-1} \right]^{-1}. \quad (29)$$

Our fiducial model is the standard Λ CMB cosmological model with the physical baryon density $\Omega_b h^2 = 0.022$, the physical dark matter density $\Omega_{cdm} h^2 = 0.11$, the ratio of the sound horizon distance to the angular diameter distance $\theta_s = 1.04$, the reionization optical depth $\tau = 0.085$, the scalar spectral index $n_s = 0.96$ and the curvature fluctuations amplitude $A_S^2 = 2.28 \times 10^{-9}$ at pivot scale $k=0.01 \text{Mpc}^{-1}$ (Dunkley et al. 2009; Komatsu et al. 2009). We present in Fig. 1 the CMB angular power spectra of the the fiducial Λ CMB cosmological model and the temperature and polarization noise power spectra obtained for the PLANCK experimental characteristics presented in Table 1 considering a coverage of the sky of 80%. The final evaluation of the systematic effects that could remain in the PLANCK data after data reduction affecting scientific exploitation will come from accurate in-flight analyses and extensive Monte Carlo simulations and is out of the scope of this work. On the other hand, we include in this study also a degradation of PLANCK ideal sensitivity possibly introduced

by residuals of systematic effects at low multipoles, where the cross-check for systematics possible at high multipoles comparing different sky areas is obviously not feasible. The most critical source of contamination will likely come from the straylight, e.g. the signal entering far sidelobes (Sandri et al. 2004) at large angular distance from the main beam. Two different sources mainly contribute to this effect: the CMB dipole (Burigana et al. 2004) and the Galactic emission (Burigana et al. 2006). The former affects only even multipoles, but it is larger in amplitudes at the considered frequencies, the latter is smaller in amplitudes, but affect all multipoles. Our simple conservative toy model, based on the above studies, assumes an increasing of the noise power at low multipoles coming from residuals of the angular power spectra estimated for these systematic effects possible generated by a non perfect subtraction of them, as in the case in which the properties of PLANCK optical response in the far sidelobes is known only with an accuracy of about 30%.

The uncertainty added to the instrumental (receiver) noise is clearly visible in Fig. 1.

We evaluate the likelihood function for 4-D and 5-D inflationary models by using the public packages COSMOMC and CAMB (Lewis & Bridle 2000; Lewis et al. 1999) modified to enable us to include the corresponding Hamilton-Jacobi formalism as described in the previous section. We perform the analysis in the framework of the flat Λ CDM standard cosmological model.

For 4-D inflation case, the Λ CDM standard cosmological model is described by the following sets of parameters receiving uniform priors:

$$\Omega_b h^2, \Omega_c h^2, \theta_s, \tau, A_S^2, \frac{H'^2}{H^2}, \frac{H''}{H}, \frac{H''' H'}{H^2}$$

where H' , H'' and H''' are the derivatives of the Hubble expansion rate H with respect to the scalar field. As noted before by Lesgourgues et al. (2008), because the physical effects in the primordial power spectra depend on combinations of Hubble expansion rate derivatives, the basis of parameters receiving uniform priors should consists in functions of the above combinations or linear combinations of them, ensuring that Markov Chains can converge in a reasonable amount of time.

By analogy, we take for 5-D inflation case the following basis of parameters receiving uniform priors:

$$\Omega_b h^2, \Omega_c h^2, \theta_s, \tau, A_S^2, \frac{y'^2}{y^2}, \frac{y''}{y}, \frac{y''' y'}{y^2}, \mu$$

where y' , y'' and y''' are the derivatives with respect to the scalar field of the parameter $y(\phi)$ defined by Eq.(12). One should note that the 5-D inflation case requires the additional parameter μ that controls the hierarchy of 4-D and 5-D Planck mass scales through the brane tension λ :

$$\mu = \frac{m_5^3}{m_4} = \sqrt{\frac{4\pi\lambda}{3}}. \quad (30)$$

We run 32 Monte Carlo chains per model and dataset, imposing for each case the Gelman & Rubin convergence criterion (Gelman & Rubin 1992).

5. The results: analysis and interpretation

5.1. The 4-D and 5-D inflationary parameter bounds

The parameter bounds derived from each set of chains are given in Table 2 while Fig. 2 and Fig. 3 show the results of our fits of 4-D and 5-D inflationary models on WMAP5+SN+BAO dataset and PLANCK-like simulated dataset. All parameters are computed at the Hubble radius crossing $k_*=0.01\text{Mpc}^{-1}$.

From the fit of 4-D inflation model to WMAP5+SN+BAO dataset we obtain bounds on n_s , A_S^2 , α_S and R at $k_* = 0.01 \text{ Mpc}^{-1}$ that translated into bounds at $k_* = 0.002 \text{ Mpc}^{-1}$ show a good agreement with bounds on the similar parameters reported by the WMAP team (Komatsu et al. 2009). Although our computation does not involve the HSR approximation in the computation of perturbations spectra, our constraints on the inflationary parameters obtained from the fit of 4-D inflation model to WMAP5+SN+BAO dataset are in general in agreement with the similar results obtained by using the HSR formalism to recover the inflationary potential, when imposing constraints on the number of e -folds during inflation (Peiris & Easther 2006a; Peiris & Easther 2006b). Our results are directly comparable with the results presented in Hamann et al. (2008) that uses the same numerical evaluation of the spectra to obtain constraints on the inflationary parameter by using a selection of CMB data including WMAP complemented by LSS measurements.

Looking at Fig. 2 and Fig. 3 we see that the amplitude of scalar power spectrum A_S^2 obtained from both datasets is suppressed in the 5-D inflation case, when compared with the similar values obtained in 4-D standard inflation. Moreover, in 5-D inflation model the joint confidence regions of the scalar spectral index n_s and tensor to scalar amplitude ratio R are anti-correlated, while the amplitude of the tensor power spectrum A_T^2 is increased, when compared with the 4-D standard inflation case. This can be attributed to a larger contribution of the tensor modes to the primordial perturbations in braneworld inflation. In this case the normalization of the scalar perturbation is reduced to obtain the correct value of R . Likewise, we obtain a strong correlation between the values of R and the tensor spectral index n_T from the fits of 4-D and 5-D inflation models to both datasets, in good agreement with the predictions of consistency relation given in Eq. (1).

Fig. 4 presents the constraints on HSR parameters derived from the fits of 4-D and 5-D inflationary models on WMAP5+SN+BAO dataset and PLANCK-like simulated dataset. We show the division of ϵ_H - η_H plane into large field, small field and hybrid field classes of

inflation models (Kinney 2002; Liddle & Taylor 2002) overlaid with our constraints on their joint 68% and 95% confidence intervals. We see that all three classes of inflation models are allowed at $2\text{-}\sigma$ level by the fit of 4-D standard inflation to our datasets.

The joint marginalized distribution of ϵ_H and η_H obtained from the fit of 5-D inflation model shows that the large field and small field classes of inflationary models are allowed by WMAP5+SN+BAO and by PLANCK datasets at $2\text{-}\sigma$ level, while the hybrid class of inflationary models seems to be disfavored by both datasets in the 5-D single-field inflation scenario. The parameter values within each class of allowed inflationary models are tightly constrained by PLANCK dataset.

Of particular interest are the differences between the degeneracy directions in $\epsilon_H\text{-}\eta_H$ plane found from the fit of 4-D inflation model to WMAP5+SN+BAO dataset and PLANCK dataset that arise due to the dependence of α_s on ξ_H^2 . The role of the ξ_H^2 in the dynamics of inflation is discussed in details in (Chongchitnan & Efstathiou 2005; Easther & Peiris 2006) and the accuracy of slow-roll inflation models with significant running is probed by using Monte Carlo reconstruction in (Easther & Kinney 2003; Makarov 2005; Peiris & Easther 2006b).

Looking at Fig. 4 one can see the preference of WMAP5+SN+BAO dataset for large and positive ξ^2 values in 4-D standard inflation case, that translates into large negative values of the running of scalar spectral index α_s and a larger degeneracy in $n_s\text{-}\alpha_s$ plane, when compared to the similar results obtained from the fit to PLANCK dataset (see Fig. 2).

The differences between the degeneracy directions obtained in 4-D standard inflation case and 5-D inflation arise via the dependence of HSR parameters on the dynamical equations driving inflation, which are different in 4-D and 5-D inflationary models.

5.2. Reconstruction of 4-D and 5-D inflationary potential

The aim in the reconstruction of the inflationary potential is to take the measurements of various inflationary observables corresponding to a particular wavenumber k and to use them to obtain the inflationary potential $V(\phi)$ and its derivatives at the scalar field value ϕ_* when the scale k crosses the Hubble radius k_* during inflation.

In the general case of the single-field braneworld inflation, the slope and the curvature of the 5-D inflationary potential as function of inflationary observables R and n_s and on the combination V/λ are given by (Liddle & Taylor 2002):

$$\frac{V'}{V} = \sqrt{\frac{16\pi R}{m_4^2}} \left[\frac{1 + V/2\lambda}{G(V/\lambda)} \right], \quad (31)$$

$$\frac{V''}{V} = \frac{4\pi}{m_4^2} \left(1 + \frac{V}{2\lambda} \right) \left[6R \frac{1 + V/\lambda}{G^2(V/\lambda)} + (n_s - 1) \right], \quad (32)$$

where:

$$G(x) = \left[\sqrt{1+x^2} - x^2 \sinh^{-1} \frac{1}{x} \right]^{-1/2}. \quad (33)$$

In the high-energy limit ($V \gg \lambda$) the function $G^2(V/\lambda) \rightarrow 3V/2\lambda$. In the low-energy limit ($\lambda \gg V$) $G^2(V/\lambda) \rightarrow 1$ and the scalar and tensor perturbation spectra of 4-D standard inflation are recovered.

We compute the magnitude, the slope and the curvature of the inflationary potential from the fits of 4-D and 5-D inflation models to our datasets by using Eq.(10) and Eq.(18) respectively. In Fig. 5 we show the allowed regions of the recovered magnitude of the inflationary potential, its slope and curvature from the fit of 4-D and 5-D inflation models to WMAP5+SN+BAO dataset and PLANCK-like simulated dataset. We also show the 1D marginal distribution of the recovered inflationary potential, its slope and curvature as a function of V/λ , obtained from the fit of 5-D inflation model to the same datasets.

Fig. 5 explicitly demonstrates the effect of the braneworld reconstruction of the inflationary potential. As V/λ is increased the magnitude and the curvature of the inflationary potential are decreased while its slope steepens. Also, the magnitude, the slope and the curvature of the inflationary potential are increased in both 4-D and 5-D inflationary scenarios when R increases.

The results from the fit of 5-D inflation model to WMAP5+SN+BAO dataset and PLANCK-like simulated dataset show that the magnitude and the slope of the inflationary potential are anti-correlated with the scalar spectral index, n_s .

The mean values of the magnitude, slope and curvature of the inflationary potentials together with their 95% upper and lower intervals are given in Table 2.

In Fig. 6 we show the dependence of the reconstructed regions of 4-D and 5-D inflationary potentials allowed by the same datasets (at 65% CL) in an observational inflationary window corresponding to $\Delta N = 11$ e -folds, as functions of the scalar field.

5.3. The 4-D and 5-D single-field inflation consistency relations

There is an infinite hierarchy of consistency equations of the single-field standard inflation (Lidsey et al. 1997; Song & Knox 2003; Chung et al. 2003; Chung & Romano 2006; Cortés & Liddle 2006). To the leading order in the slow-roll approximation, the consistency relation of the standard scenario given in Eq.(1) is degenerate. To next-to-leading order, this consistency relation receives corrections of the form (Copeland et al. 1994; Lidsey et al. 1997):

$$n_T = -2 \frac{A_T^2}{A_S^2} \left[1 - \frac{A_T^2}{A_S^2} + (1 - n_S) \right], \quad (34)$$

that do not depend on the spectral index of the tensor perturbations.

As the inflationary observables n_S , n_T and R are evaluated at the epoch of horizon-crossing quantified by the number of e -folds N before the end of the inflation at which our present Hubble scale equalled the Hubble scale during inflation, the uncertainties in the determination of N translates to theoretical errors in the determination of the inflationary observables. Assuming that the ratio of the entropy per comoving interval today to that after reheating is negligible, the main uncertainty in the determination of N is caused by our ignorance in the determination of the reheating temperature after inflation leading to an error of $\Delta N \sim 14$ (Kinney & Riotto 2006; Adshead & Easther 2008).

In order to test the observational signature that standard and braneworld inflationary scenarios may produce, we use the estimates of the inflationary parameters obtained from the fits to WMAP5+SN+BAO and PLANCK-like simulated datasets to compare the experimental difference between tensor spectral indexes, $n_T^{4D} - n_T^{5D}$, to the theoretical error in the tensor spectral index computed by using the consistency relation (34).

To the lowest order in slow-roll parameters, the uncertainties ΔR and Δn_S in terms of the uncertainty in the number of e -folds ΔN are given by (Kinney 2002; Kinney et al. 2004):

$$\frac{\Delta R}{\Delta N} = R \left[(n_S - 1) + \frac{R}{8} \right], \quad (35)$$

$$\frac{\Delta n_S}{\Delta N} = -\frac{5}{16}R(n_S - 1) - \frac{3}{32}R^2 + 2\xi^2. \quad (36)$$

The theoretical uncertainty on the tensor spectral index in the standard 4-D inflation can be straightforwardly obtained from Eq.(34) by using Eqs.(35) and (36):

$$\frac{\Delta n_T^c}{\Delta N} = \frac{1}{4} \left[1 - \frac{n_S}{2} - \frac{A_T^2}{A_S^2} \right] \frac{\Delta R}{\Delta N} + \frac{1}{8} \frac{A_T^2}{A_S^2} \frac{\Delta n_S}{\Delta N}. \quad (37)$$

The estimate of $\Delta n_T^c/\Delta N$ should be compared to $\Delta n_T = n$. In Table 3 we present the mean values of the lowest order estimates of the theoretical errors $\Delta R/R$, $\Delta n_S/n_S$ and Δn_T^c from the fit of 4-D inflation model to WMAP5+SN+BAO and PLANCK datasets obtained by assuming $\Delta N=14$ e -folds and the mean values of the difference between the experimental values of the tensor spectral indexes $\Delta n_T = n_T^{4D} - n_T^{5D}$, while in Fig. 7 we show their 1D marginalized likelihood probability distributions. We also show in the same figure the 1D marginalized likelihood probability distribution of the lowest order estimates of the theoretical errors Δn_T^c , obtained by assuming $\Delta N=14$, compared with the 1D marginalized likelihood probability distribution of the difference $\Delta n_T = n_T^{4D} - n_T^{5D}$ and their 2D joint allowed bounds (at 68% and 95% CL).

The analysis of the results presented in Fig. 7 and Table 3 shows that the Δn_T parameter space obtained from the fits of 4-D and 5-D inflation models to WMAP5+SN+BAO dataset

is dominated by the theoretical error Δn_T^c : the confidence interval corresponding to Δn_T^c is smaller by a factor of 1.2 than that corresponding to Δn_T . The same parameter space is better constrained by the PLANCK dataset: in this case the confidence interval corresponding to Δn_T^c is three times smaller than that corresponding to Δn_T .

We conclude that the detection of tensor perturbations and the theoretical uncertainties in the inflationary observable represent a significant challenge for the future PLANCK CMB measurements: distinguishing between the observational signatures of the standard and braneworld single-field inflation scenarios.

6. Conclusions

One of the most anticipated results of forthcoming PLANCK high precision CMB measurements is probing the physics of inflation and in particular, the reconstruction of the inflation potential. On the other hand, the possibility that our four-dimensional Universe could lie on a brane embedded in a higher dimensional space has important consequences for the early universe and in particular for the cosmological inflation.

In this paper we make a more general determination of the inflationary observables in the 4-D and 5-D single-field inflationary scenarios by exact reconstruction of the dynamics of the inflation potential during the observable inflation, with a minimal number of assumptions.

Making use of the general formalism for 5-D single-field inflation developed by Hawkins and Lidsey (Hawkins & Lidsey 2001; Hawkins & Lidsey 2003) valid in all regimes, having many of the properties of the *Hamilton-Jacobi* formalism developed for the 4-D standard inflation, we compute the scale dependence of the amplitudes of the scalar and tensor perturbations by integrating the exact mode equation. Our computation does not assume the slow-roll approximation and is valid in all regimes if the field is monotonically rolling down its potential. The solutions in 4-D and 5-D inflation scenarios differ through the dynamics of the background scalar field and the number of e -folds assumed to be compatible with the observational window of inflation.

We address higher-order effects in the standard and braneworld single-field inflation scenarios by fitting the Hubble expansion rate $H(\phi)$ and subsequently the inflationary potential $V(\phi)$, directly to WMAP5+SN+BAO and Planck-like simulated datasets.

One should note that our results refer to the initial scalar and tensor perturbation spectra and not to the braneworld effects on the subsequent evolution of the perturbations that is likely to be model dependent (Leong et al. 2002; Rhodes et al. 2003).

Assuming that the ratio of the entropy per comoving interval today to that after reheating

is negligible, we analyze the implications of the theoretical uncertainty in the determination of the reheating temperature after inflation on the observable predictions of inflation.

We find that the detection of tensor perturbations and the theoretical uncertainties in the inflationary observables represent a significant challenge for the future PLANCK CMB measurements: distinguishing between the observational signatures of the standard and braneworld single-field inflation scenarios.

We acknowledge the use of the GRID computing system facility at the Institute for Space Sciences Bucharest and to the staff working there.

L.P and A.C. are partially supported by ESA/PECS Contract C98051 and CNCSIS Contract 539/2009.

Table 1. The expected experimental characteristics for the PLANCK frequency channels considered in the paper (Mandolesi et al. 2009; PLANCK Consortia 2005). Δ_T and Δ_P are the sensitivities per pixel for temperature and polarization maps.

Frequency (ν) (GHz)	FWHM (arc-minutes)	Δ_T (μK)	Δ_P (μK)
70	13	23.48	33.21
100	9.5	6.8	10.9
143	7.1	6.0	11.4

Table 2. The mean values and 95% CL lower and upper intervals of the derived parameters obtained from the fit of 4-D and 5-D inflation models to WMAP5+SN+BAO dataset and PANCK-like simulated dataset. All parameters are computed at the Hubble radius crossing $k_*=0.01 \text{ Mpc}^{-1}$.

Parameter	WMAP5+SN+BAO		PLANCK	
	4-D Inflation	5-D Inflation	4-D Inflation	5-D Inflation
$\Omega_b h^2$	0.022 ^{0.023} _{0.021}	0.022 ^{0.023} _{0.021}	0.022 ^{0.023} _{0.021}	0.022 ^{0.023} _{0.021}
$\Omega_c h^2$	0.111 ^{0.117} _{0.106}	0.111 ^{0.117} _{0.106}	0.113 ^{0.122} _{0.112}	0.112 ^{0.123} _{0.111}
τ	0.082 ^{0.109} _{0.055}	0.080 ^{0.106} _{0.056}	0.081 ^{0.897} _{0.734}	0.081 ^{0.903} _{0.073}
θ_s	1.039 ^{1.045} _{1.034}	1.039 ^{1.044} _{1.034}	1.050 ^{1.051} _{1.048}	1.053 ^{1.053} _{1.051}
$\ln[10^{10} A_S^2]$	3.143 ^{3.201} _{3.083}	3.061 ^{3.137} _{2.986}	3.172 ^{3.194} _{3.146}	3.103 ^{3.142} _{3.077}
ϵ_H	< 0.035	< 0.024	< 0.019	< 0.017
η_H	0.011 ^{0.051} _{-0.022}	-0.008 ^{0.011} _{-0.022}	-0.006 ^{0.013} _{-0.022}	-0.009 ^{0.011} _{-0.019}
ξ^2	0.007 ^{0.017} _{-0.006}	0.001 ^{0.011} _{-0.003}	-0.001 ^{0.011} _{-0.006}	0.001 ^{0.008} _{-0.007}
n_S	0.956 ^{0.979} _{0.932}	0.947 ^{0.995} _{0.906}	0.958 ^{0.964} _{0.948}	0.968 ^{1.058} _{0.940}
α_S	-0.012 ^{0.021} _{-0.038}	-0.006 ^{0.007} _{-0.021}	-0.005 ^{0.006} _{-0.022}	0.000 ^{0.021} _{-0.015}
n_T	> -0.042	> -0.055	> -0.028	> -0.043
$\ln[10^{10} A_T^2]$	-1.174 ^{-0.203} _{-3.071}	-0.836 ^{1.477} _{-3.095}	-2.867 ^{-1.042} _{-5.501}	-0.448 ^{2.018} _{-2.983}
R	< 0.556	< 0.476	< 0.278	< 0.220
V/λ	-	8.131 ^{20.632} _{0.002}	-	3.519 ^{6.383} _{0.002}
$10^{11} \times V m_4$	1.511 ^{3.004} _{0.174}	1.342 ^{2.783} _{0.244}	0.449 ^{1.434} _{0.001}	0.933 ^{2.131} _{0.088}
$(V'/V)m_4^2$	0.895 ^{1.301} _{0.329}	0.922 ^{1.307} _{0.402}	0.423 ^{0.871} _{0.090}	0.680 ^{1.057} _{0.222}
$(V''/V)m_4^2$	0.619 ^{2.051} _{-0.848}	-0.683 ^{1.195} _{-0.265}	0.356 ^{1.116} _{-0.014}	-0.479 ^{0.774} _{-1.437}

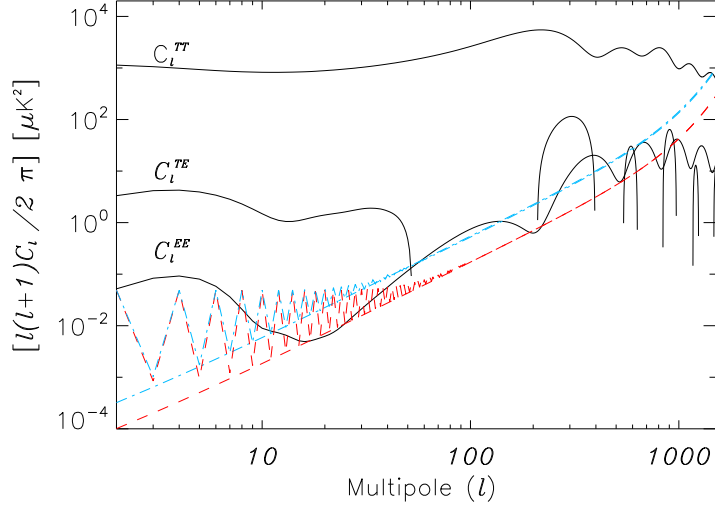


Fig. 1.— The CMB angular power spectra of the fiducial Λ CMB cosmological model and the temperature (dashed red line) and polarization (dash-dotted blue line) noise power spectra obtained for the PLANCK experimental characteristics presented in Table 1, considering a coverage of the sky of 80%.

Table 3. The mean values and 95% CL lower and upper intervals of the lowest order estimates of the theoretical errors $\Delta R/R$, $\Delta n_S/n_S$ and Δn_T^c obtained from the fit of 4-D inflation model to WMAP5+SN+BAO and PLANCK datasets by assuming $\Delta N=14$, and the mean values and 95% CL lower and upper intervals of $\Delta n_T = n_T^{4D} - n_T^{5D}$, obtained from the fits of 4-D and 5-D inflation models to the same datasets.

	WMAP5+SN+BAO	PLANCK
$\Delta R/R$	$-0.115_{-0.727}^{0.493}$	$0.177_{-0.061}^{0.478}$
$\Delta n_S/n_S$	$0.104_{-0.352}^{0.512}$	$-0.006_{-0.140}^{0.140}$
Δn_T^c	$-0.002_{-0.045}^{0.032}$	$-0.004_{-0.022}^{0.000}$
$\Delta n_T = n_T^{4D} - n_T^{5D}$	$-0.003_{-0.048}^{0.049}$	$0.003_{-0.026}^{0.043}$

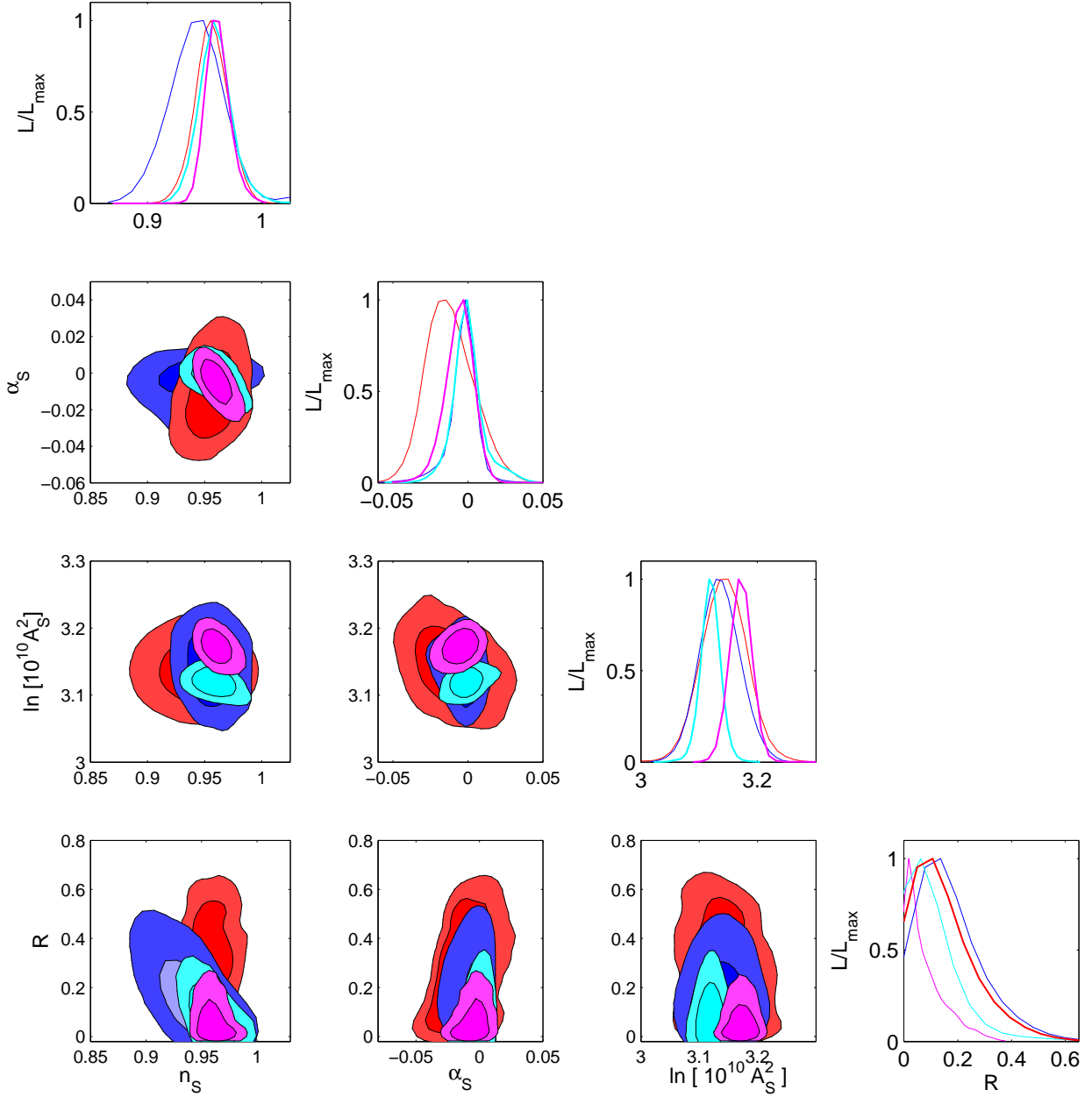


Fig. 2.— We show the results of the fits to the WMAP5+SN+BAO dataset of 4-D inflation model in red and 5-D in inflation model in blue. The results of the fits to the PLANCK-like simulated dataset of 4-D inflation model are in magenta and of 5-D in inflation model are in cyan. The top plot in each column shows the probability distribution of different scalar inflationary observables while the other plots show their joint 68% and 95% confidence intervals. All parameters are computed at the Hubble radius crossing $k_*=0.01\text{Mpc}^{-1}$.

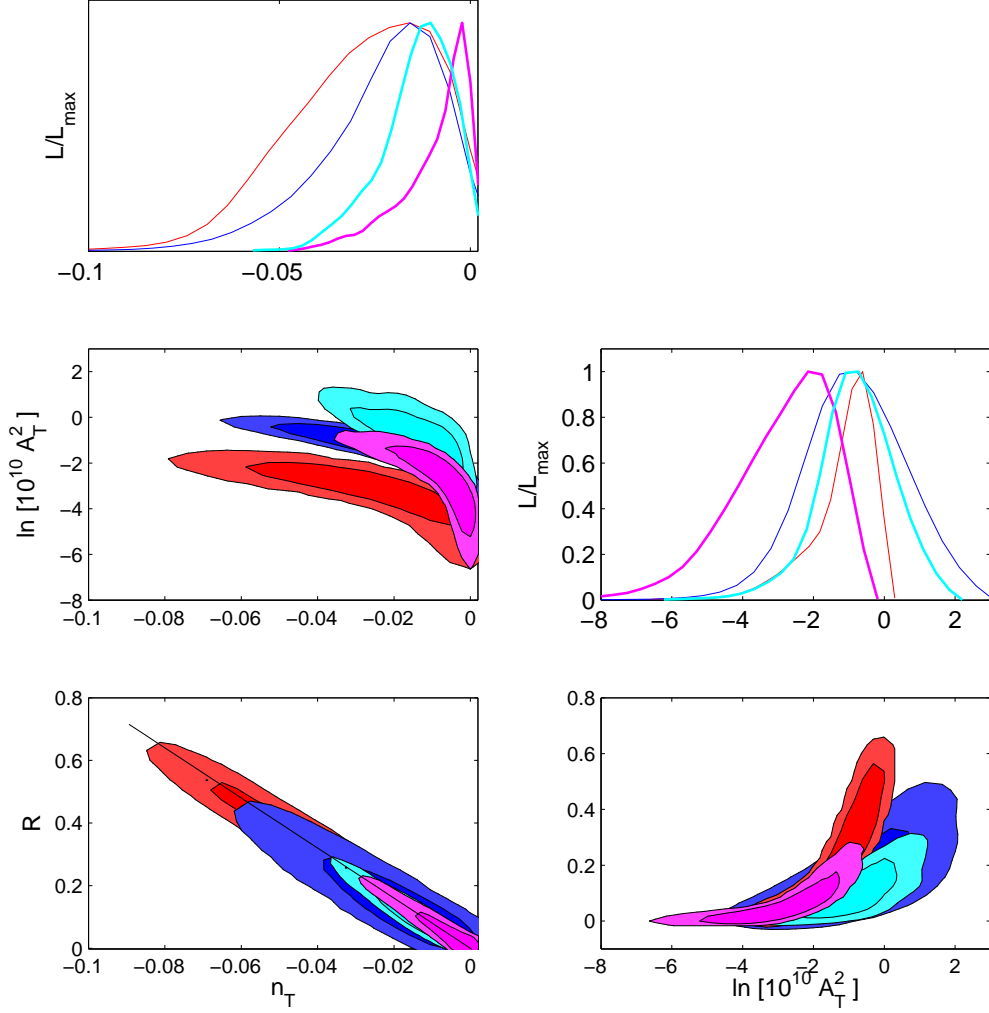


Fig. 3.— We show the results of the fits to the WMAP5+SN+BAO dataset of 4-D inflation model in red and of 5-D in inflation model in blue. The results of the fits to the PLANCK-like simulated dataset of 4-D inflation model are in magenta and of 5-D in inflation model are in cyan. The top plot in each column shows the probability distribution of different tensorial inflationary observables while the other plots show their joint 68% and 95% confidence intervals. All parameters are computed at the Hubble radius crossing $k_*=0.01\text{Mpc}^{-1}$.

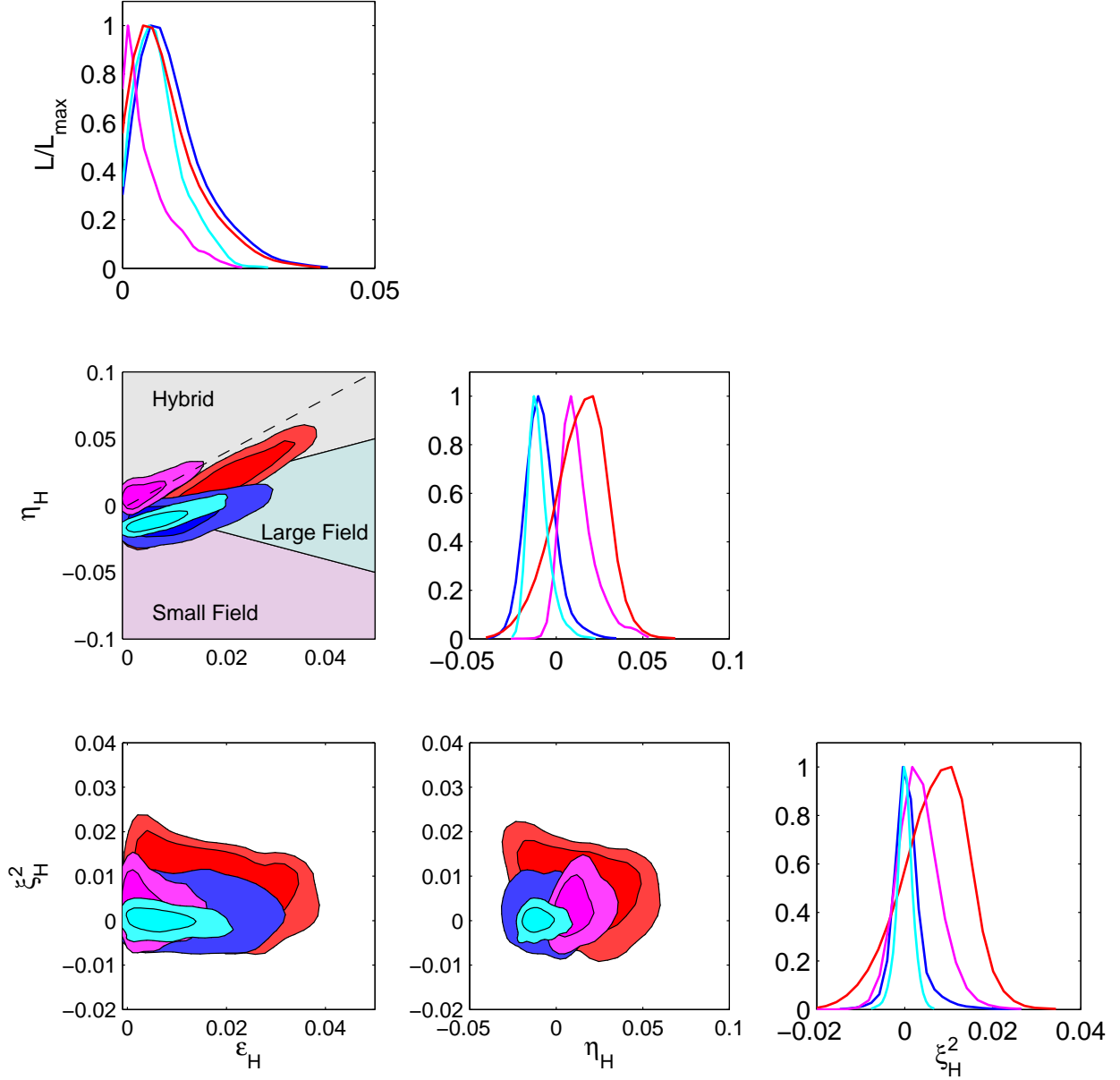


Fig. 4.— We show the bounds on the HSR parameters derived from the fits to WMAP5+SN+BAO dataset of 4-D inflation model in red and of 5-D inflation model in blue. The results of the fits to the PLANCK-like simulated dataset of 4-D inflation model are in magenta and of 5-D in inflation model are in cyan. The top plot in each column shows the probability distribution of different HSR parameters while the other plots show their joint 68% and 95% confidence intervals. All parameters are computed at the Hubble radius crossing $k_*=0.01\text{Mpc}^{-1}$. We show the division of $\epsilon_H - \eta_H$ plane into large field ($-\epsilon_H < \eta_H < \epsilon_H$), small field ($\eta_H < -\epsilon_H$) and hybrid field ($0 < \epsilon_H < \eta_H$) classes of inflation models.

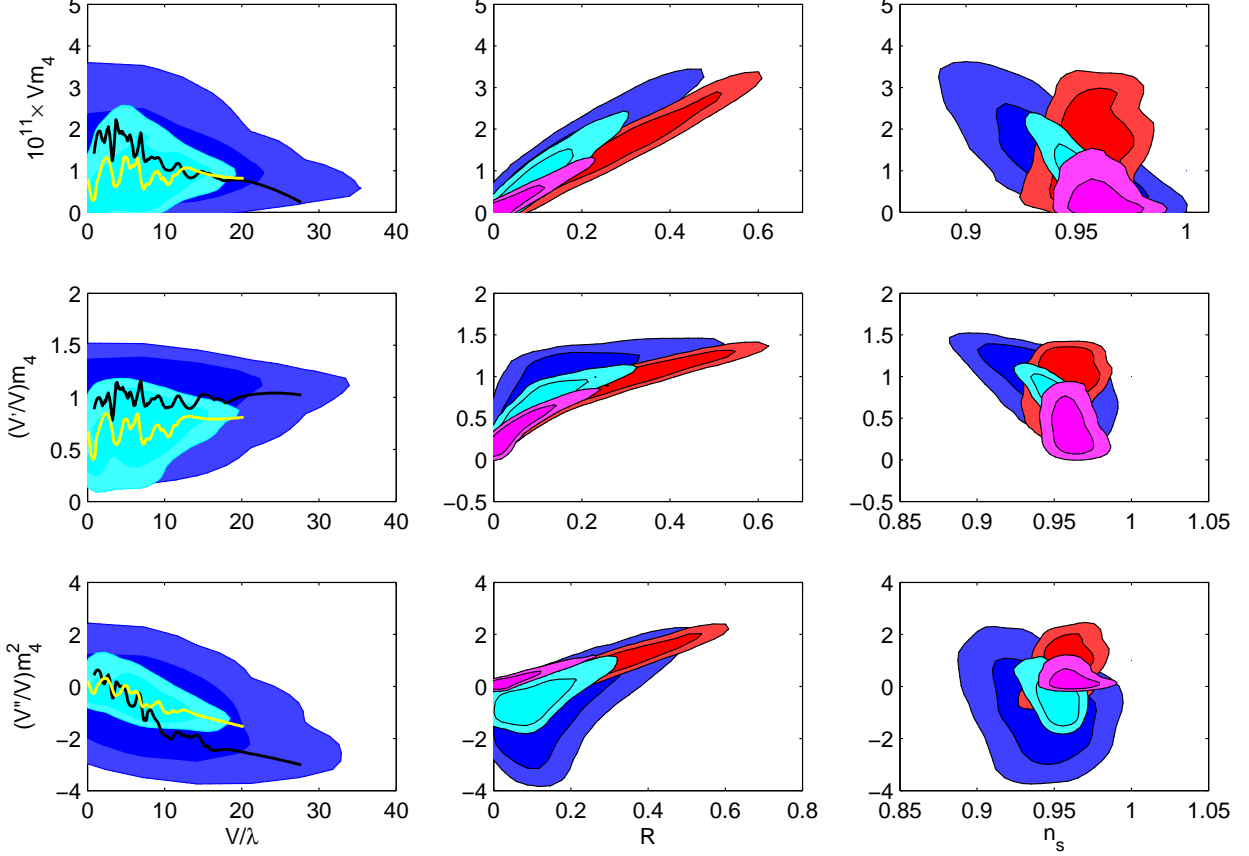


Fig. 5.— We present the recovered regions (at 68% and 95% CL) of the magnitude, slope and curvature of the inflationary potential from the fits to WMAP5+SN+BAO dataset of 4-D inflation model in red and of 5-D inflation model in blue. The similar results from the fits to PLANCK-like simulated dataset of 4-D inflation model are in magenta and of 5-D in inflation model are in cyan. We also show the 1D marginal distribution of the recovered magnitude of the inflationary potential, its slope and curvature (at 95% CL) as function of V/λ obtained from the fit of 5-D inflation model to WMAP5+SN+BAO dataset (black lines) and PLANCK-like simulated dataset (yellow lines). All parameters are computed at the Hubble radius crossing $k_*=0.01\text{Mpc}^{-1}$.

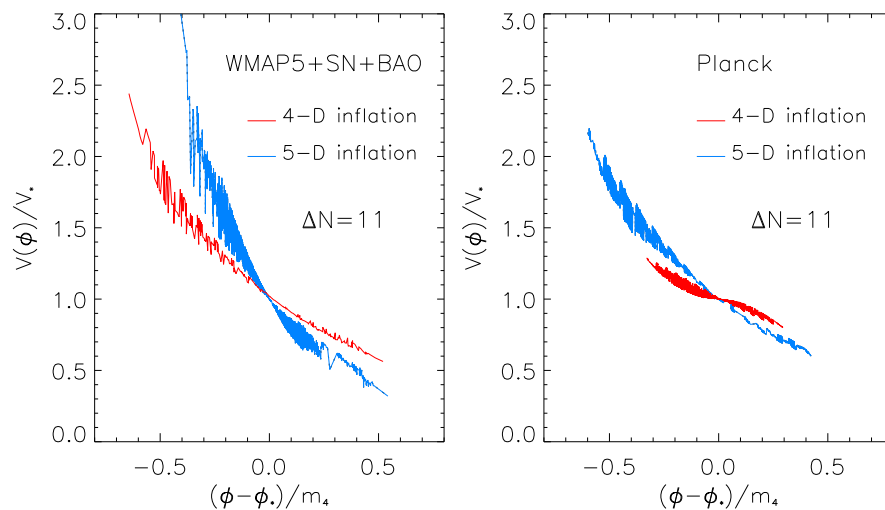


Fig. 6.— We present the regions of 4-D and 5-D inflationary potentials allowed at 65% CL by WMAP5+SN+BAO and PLANCK-like simulated datasets in the same observational inflation window corresponding to $\Delta N = 11$ e -folds. For each case, the magnitude of inflationary potential is normalized to V_* , the value of the inflationary potential at Hubble radius crossing $k_* = 0.01 \text{Mpc}^{-1}$.

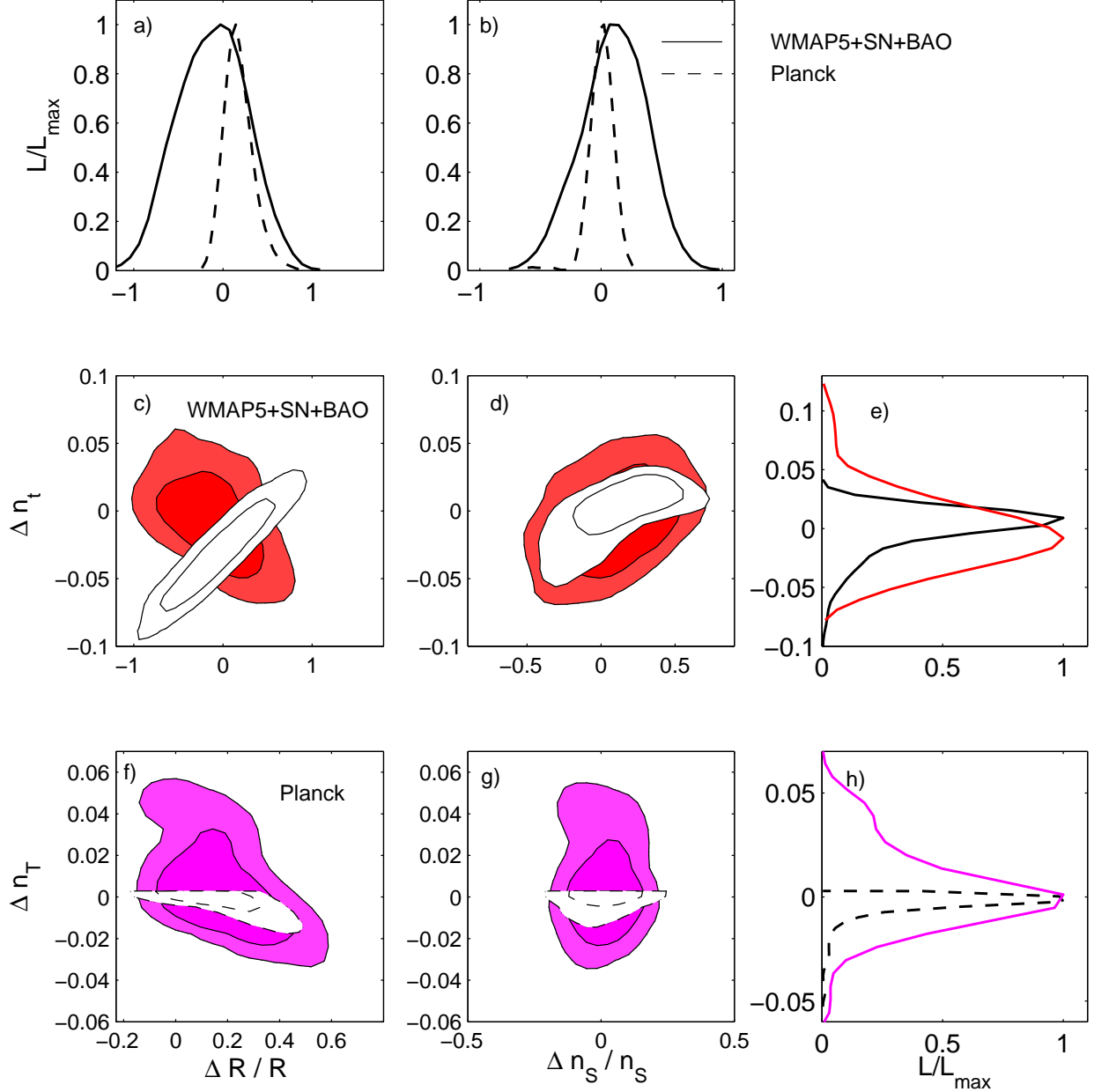


Fig. 7.— Panels a) and b): 1D marginalized likelihood probability distributions of the theoretical errors $\Delta R/R$ and $\Delta n_S/n_S$ obtained from the fits of 4-D standard inflation model to WMAP5+SN+BAO dataset (continuous line) and PLANCK dataset (dashed line) assuming $\Delta N=14$. Panels c) and d): 2D joint marginalized probability distributions (at 68% and 95% CL) obtained from the fits to WMAP4+SN+BAO dataset. The red filled contours corresponds to $\Delta n_T = \Delta n_T^{4D} - \Delta n_T^{5D}$ and the white filled contours corresponds to the theoretical error Δn_T^c obtained by assuming $\Delta N=14$. Panel e): 1D marginalized likelihood probability distributions of Δn_T^c (black continuous line) and $\Delta n_T = n_T^{4D} - n_T^{5D}$ (red continuous line) obtained from the fits to WMAP5+SN+BAO dataset. Panels e) and g): 2D joint marginalized probability distributions (at 68% and 95% CL) obtained from the fits to PLANCK-like simulated dataset. The magenta filled contours corresponds to $\Delta n_T = \Delta n_T^{4D} - \Delta n_T^{5D}$ and the white filled contours corresponds to the theoretical error Δn_T^c obtained by assuming $\Delta N=14$. Panel h): 1D marginalized likelihood probability distributions of Δn_T^c (black dashed line)

REFERENCES

- Abbott, L. F. & Wise, M. B. 1984, Nucl. Phys. B, 244, 541
- Alabidi, L. & Lidsey, J. E. 2008, Phys. Rev. D, 78, 103519 [arXiv:0807.2181]
- Albrecht, A. & Steinhardt, P. J. 1982, Phys. Rev. Lett., 48, 1220
- Adshead, P. & Easther, R. 2008, J. Cosmology Astropart. Phys., 10, 047 [arXiv:0802.3898]
- Bardeen, J. M., Steinhardt, P. J. & Turner, M. S. 1983, Phys. Rev. D, 28, 679
- Binetruy, P., Deffayet, C., Ellwanger, U., Langlois, D. 2000, Phys. Lett. B, 477, 285 [arXiv:hep-th/9910219]
- Burigana, C., Sandri, M., Villa, F., Maino, D., Paladini, R., Baccigalupi, C., Bersanelli, M., Mandolesi, N. 2004, A&A, 428, 311 [arXiv:astro-ph/0303645]
- Burigana, C., Gruppuso, A., Finelli, F. 2006, MNRAS, 371, 1570-1586 [arXiv:astro-ph/0607506]
- Calcagni, G. 2003, J. Cosmology Astropart. Phys., 11, 009 [arXiv:hep-ph/0310304]
- Calcagni, G. 2004, J. Cosmology Astropart. Phys., 06, 002 [arXiv:hep-ph/0312246].
- Chongchitnan, S. & Efstathiou, G. 2005, Phys. Rev. D, 72, 083520 [arXiv:astro-ph/0508355].
- Chung, D. J. H., Shiu, G. & Trodden, M. 2003, Phys. Rev. D, 68, 063501 [arXiv:astro-ph/0305193].
- Chung, D. J. H. & Romano, A. E. 2006, Phys. Rev. D, 73, 103510 [arXiv:astro-ph/0508411].
- Copeland, E. J., Kolb, E. W., Liddle, A. R., Lidsey, J. E. 1994, Phys. Rev. D, 49, 1840 [arXiv:astro-ph/9308044]
- Cortês, M. & Liddle, A. R. 2006, Phys. Rev. D, 73, 083523 [arXiv:astro-ph/0603016]
- Dunkley, J., et al. 2009, ApJS, 180, 306 [arXiv:0803.0586]
- Easther, R. & Kinney, W. H. 2003, Phys. Rev. D, 67, 043511 [arXiv:astro-ph/0210345]
- Easther, R. & Peiris, H. V. 2006, J. Cosmology Astropart. Phys., 09, 010 [arXiv:astro-ph/0604214]
- Gelman, A. & Rubin, D. 1992, Statistical Science, 7, 457

- Guth, A. H. 1981, Phys. Rev. D, 23, 347
- Guth, A. H. & Pi S. Y. 1982, Phys. Rev. Lett., 49, 1110
- Hamann, J., Lesgourgues, J., Valkenburg, W. 2009, J. Cosmology Astropart. Phys., 04, 016 [arXiv:0802.0505]
- Hawking, S. W. 1982, Phys. Lett. B, 115, 295
- Hawkins, R. M. & Lidsey, J. E. 2003, Phys. Rev. D, 63, 041301 [arXiv:gr-qc-ph/0011060]
- Hawkins, R. M. & Lidsey, J. E. 2003, Phys. Rev. D, 68, 083505 [arXiv:astro-ph/0306311]
- Horava, P. & Witten, E., 1996, Nucl. Phys B, 475, 94 [arXiv:hep-th/9603142]
- Kinney, W. H. 2002, Phys. Rev. D, 64, 5 [arXiv:astro-ph/0206032]
- Kinney, W. H. & Riotto, A. 2006, J. Cosmology Astropart. Phys., 03, 011 [arXiv:astro-ph/0511127]
- Kinney, W. H., Kolb, E. W., Melchiorri, A., Riotto, A. 2004, Phys. Rev. D, 69, 103516 [arXiv:hep-ph/0305130]
- Kobayashi, T., Kudoh, H. & Tanaka, T. 2004, Phys. Rev. D, 68, 044025 [arXiv:gr-qc/0305006]
- Komatsu, E. et al., 2009, ApJS, 180, 330 [arXiv:0803.0547]
- Kowalski, M., et al. (Supernova Cosmology Project) 2008, ApJ, 686, 749 [arXiv:0804.4142]
- Koyama, K., Langlois, D., Maartens, R., Wands, D. 2004, J. Cosmology Astropart. Phys., 11, 002 [arXiv:hep-th/0408222]
- Koyama, K., Mennim, A., Wands, D. 2005a, Phys. Rev. D72, 064001 [arXiv:hep-th/0504201]
- Koyama, K., Mizuno, S., Wands, D. 2005b, J. Cosmology Astropart. Phys., 08, 009 [arXiv:hep-th/0506102]
- Koyama, K., Mennim, A., Wands, D. 2008, Phys. Rev. D, 77, 021501 [arXiv:0709.0294]
- Langlois, D., Maartens, R., Sasaki, M., Wands, D. 2001, Phys. Rev. D, 63, 084009 [arXiv:hep-th/0012044]

- Lesgourgues, J., Starobinsky, A. A., Valkenburg, W. 2008, *J. Cosmology Astropart. Phys.*, 01, 010 [arXiv:0710.1630] ²
- Lewis, A., Challinor, A. & Lasenby A. 2000, *ApJ*, 538, 473[arXiv:astro-ph/9911177] ³
- Lewis, A. & Briddle, S. 2002, *Phys. Rev. D*, 66, 103511 [arXiv:astro-ph/0205436]⁴
- Liddle, A. R. & Turner, M. S. 1994, *ApJ*, 50, 758 [arXiv:astro-ph/9402021]
- Liddle, A. R., Parsons, P., Barrow, J. D. 1994, *Phys. Rev. D*, 50, 7222 [arXiv:astro-ph/9408015]
- Liddle, A. R. & Lyth D. H. 2000, *Cosmological inflation and large-scale structure* (Cambridge: Cambridge University Press)
- Liddle, A. & Taylor, A. N. 2002, *Phys. Rev. D*, 65, 041301 [arXiv:astro-ph/0109412]
- Liddle, A. R. & Smith, A. J. 2003, *Phys. Rev. D*, 68, 061301 [arXiv:astro-ph/0307017]
- Lidsey J. E., Liddle A.R., Kolb E.W. , Copeland E. J., Barreiro T., Abney M. 1997, *Rev. Mod. Phys.*, 69, 373 [arXiv:astro-ph/9508078].
- Lidsey, J. E. & Tavakol, R. 2003, *Phys. Lett. B*, 575, 157 [arXiv:astro-ph/0304113]
- Linde, A. D, 1982, *Phys. Lett.B*, 108, 389
- Linde, A. D. 1983, *Phys. Lett.B*, 129, 177
- Leong, B., Challinor, A., Maartens, R., Lasenby, A. 2002, *Phys. Rev. D*, 66, 104010 [arXiv:astro-ph/0208015]
- Maartens, R., Wands, D., Bassett, B. A., Heard, I. P. C. 2000, *Phys. Rev. D*, 62, 041301 [arXiv:hep-ph/9912464]
- Maartens, R. 2004, *Liv. Rev. Rel.*, 7, 7 [arXiv:gr-qc/0312059]
- Makarov, A. 2005, *Phys. Rev. D*, 72, 083517 [arXiv:astro-ph/0506326].
- Mandolesi, N., Bersanelli, M., Butler, C.R., et al. 2009, *A&A*, submitted

²<http://www.lapp.in2p3.fr/valkenbu/inflationH/>

³<http://camb.info>

⁴<http://cosmologist.info/cosmomc/>

- Martin, J. & Ringeval, C. 2006, *J. Cosmology Astropart. Phys.*, 08, 009 [arXiv:astro-ph/0605367].
- Mukhanov, V. F. & Chibisov, G. V. 1981, *JETP Lett.*, 33, 532
- Mukhanov, V. F. 1985, *Zh. Pis'ma v Redaktsiiu* 41, 402 (*JETP Lett.* 41, 493)
- Mukhanov, V. F. 1989, *Phys. Lett. B*, 218, 17
- Nolta, M. et al. 2009, *ApJS*, 180, 296 [arXiv:0803.0593]
- Peiris, H. V. et al. 2003, *ApJS*, 148, 213 [arXiv:astro-ph/0302225]
- Peiris, H. V. & Easter, R. 2006a, *J. Cosmology Astropart. Phys.*, 10, 017 [arXiv:astro-ph/0609003]
- Peiris, H. V. & Easter, R. 2006b, *J. Cosmology Astropart. Phys.*, 07, 002 [arXiv:astro-ph/0603587]
- Percival, W. J., Cole, S., Eisenstein, D. J., Nichol, R. C., Peacock, J. A. Pope, A. C., Szalay, A., S. 2007, *MNRAS*, 381, 1053 [arXiv:0705.3323]
- Perotto L., Lesgourgues J., Hannestad S., Tu H., Wong Y. Y. Y., 2006, *J. Cosmology Astropart. Phys.*, 10, 013 [astro-ph/0606227]
- The Planck Consortia 2005, *ESA-SCI*, 1 [astro-ph/0604069]
- Popa L.,A. & Vasile, A. 2007, *J. Cosmology Astropart. Phys.*, 10, 017 [arXiv:0708.2030]
- Ramirez, E. & Liddle, A. R. 2004, *Phys. Rev. D*, 69, 083522 [arXiv:astro-ph/0309608]
- Randall, L., Sundrum, R. 1999a, *Phys. Rev. Lett.*, 83, 4690 [arXiv:hep-th/9906064]
- Randall, L., Sundrum, R. 1999b, *Phys. Rev. Lett.*, 83, 3370 [arXiv:hep-ph/9905221]
- Rhodes C. S., van de Bruck, C., Brax, P., Davis, A. C. 2003, *Phys. Rev. D*, 68, 083511 [arXiv:astro-ph/0306343]
- Rubakov, V. A. 2001, *Phys. Usp.*, 44, 871 [arXiv:hep-ph/0104152]
- Salopek D. S. & Bond J. R. 1990, *Phys. Rev. D*, 42, 3936
- Sandri, M., Villa, F., Nesti, R., Burigana, C., Bersanelli, M., Mandolesi, N. 2004, *A&A*, 428, 299 [arXiv:astro-ph/0305152]

- Sato, K. 1981, MNRAS, 195, 467
- Seery, D., Taylor, A. 2005, Phys. Rev. D, 71, 063508 [arXiv:astro-ph/0309512]
- Song Y. S. & Knox, L. 2003, Phys. Rev. D, 68, 043518 [arXiv:astro-ph/0305411]
- Starobinsky, A. A. 1979, JETP Lett., 30, 682
- Starobinsky, A. A. 1982, Phys. Lett. B, 117, 175
- Steinhardt, P. J. & Turner, M. S. 1984, Phys. Rev. D, 29, 2162
- Stewart, E. D., Lyth, D. H. 1993, Phys. Lett. B, 302, 171 [arXiv:gr-qc/9302019]
- Tsujikawa, S. & Liddle, A. R. 2004, J. Cosmology Astropart. Phys., 03, 001
[arXiv:astro-ph/0312162]